

Année de publication : 2018

Prado Martins R., Findakly S., Daskalogianni C., Teulade-Fichou M.P., Blondel M., Fåhræus R.
(2018 Nov 29)

In Cellulo Protein-mRNA Interaction Assay to Determine the Action of G-Quadruplex-Binding Molecules

Molecules : 23 : 3124 : [DOI : 10.3390/molecules23123124](https://doi.org/10.3390/molecules23123124)

Résumé

Protein-RNA interactions (PRIs) control pivotal steps in RNA biogenesis, regulate multiple physiological and pathological cellular networks, and are emerging as important drug targets. However, targeting of specific protein-RNA interactions for therapeutic developments is still poorly advanced. Studies and manipulation of these interactions are technically challenging and in vitro drug screening assays are often hampered due to the complexity of RNA structures. The binding of nucleolin (NCL) to a G-quadruplex (G4) structure in the messenger RNA (mRNA) of the Epstein-Barr virus (EBV)-encoded EBNA1 has emerged as an interesting therapeutic target to interfere with immune evasion of EBV-associated cancers. Using the NCL-EBNA1 mRNA interaction as a model, we describe a quantitative proximity ligation assay (PLA)-based in cellulo approach to determine the structure activity relationship of small chemical G4 ligands. Our results show how different G4 ligands have different effects on NCL binding to G4 of the EBNA1 mRNA and highlight the importance of in-cellulo screening assays for targeting RNA structure-dependent interactions.

Daniel A Fletcher, Junsang Doh, Matthieu Piel (2018 Nov 27)

Preface.

Methods in cell biology : xiii : [DOI : S0091-679X\(18\)30175-4](https://doi.org/10.1016/S0091-679X(18)30175-4)

Résumé

Verga D., Nguyen C.H., Dakir M., Coll J.L., Teulade-Fichou M.P., Molla A. (2018 Nov 20)

Polyheteroaryl Oxazole/Pyridine-based compounds selected in vitro as G-quadruplex ligands inhibit Rock kinase and exhibit antiproliferative activity

Journal of Medicinal Chemistry : 61 : 10502-10518 : [DOI : 10.1021/acs.jmedchem.8b01023](https://doi.org/10.1021/acs.jmedchem.8b01023)

Résumé

Heptaheteroaryl compounds comprised of oxazole and pyridine units (TOxaPy) are quadruplex DNA (G4)-interactive compounds. Herein, we report on the synthesis of parent compounds bearing either amino side chains (TOxaPy-1-5) or featuring an isomeric oxazole-pyridine central connectivity (iso-TOxapy, iso-TOxapy 1-3) or a bipyridine core (iso-TOxabiPy). The new isomeric series showed significant G4-binding activity in vitro and remarkably 3 compounds (iso-TOxaPy, iso-TOxaPy-1, iso-TOxabiPy) exhibited high antiproliferative activity towards a tumor panel of cancer cell lines. However, these

compounds do not behave as typical G-quadruplex binders and the kinase profiling assay revealed that the best antiproliferative molecule iso-TOxaPy selectively inhibited Rock-2. The targeting of Rock kinase was confirmed in cells by the dephosphorylation of Rock-2 substrates, the decrease of stress fibers and peripheral focal adhesions, as well as the induction of long neurite-like extensions. Remarkably two of these molecules were able to inhibit the growth of cells organized as spheroids.

Maheva Andriatsilavo, Marine Stefanutti, Katarzyna Siudeja, Carolina N Perdigoto, Benjamin Boumard, Louis Gervais, Alexandre Gillet-Markowska, Lara Al Zouabi, François Schweisguth, Allison J Bardin (2018 Nov 20)

Spn limits intestinal stem cell self-renewal.

PLoS genetics : e1007773 : [DOI : 10.1371/journal.pgen.1007773](https://doi.org/10.1371/journal.pgen.1007773)

Résumé

Precise regulation of stem cell self-renewal and differentiation properties is essential for tissue homeostasis. Using the adult *Drosophila* intestine to study molecular mechanisms controlling stem cell properties, we identify the gene *split-ends* (*spen*) in a genetic screen as a novel regulator of intestinal stem cell fate (ISC). *Spn* family genes encode conserved RNA recognition motif-containing proteins that are reported to have roles in RNA splicing and transcriptional regulation. We demonstrate that *spen* acts at multiple points in the ISC lineage with an ISC-intrinsic function in controlling early commitment events of the stem cells and functions in terminally differentiated cells to further limit the proliferation of ISCs. Using two-color cell sorting of stem cells and their daughters, we characterize *spen*-dependent changes in RNA abundance and exon usage and find potential key regulators downstream of *spen*. Our work identifies *spen* as an important regulator of adult stem cells in the *Drosophila* intestine, provides new insight to *Spn*-family protein functions, and may also shed light on *Spn*'s mode of action in other developmental contexts.

Athanasia Stoupa, Frédéric Adam, Dulanjalee Kariyawasam, Catherine Strassel, Sanjay Gawade, Gabor Szinnai, Alexandre Kauskot, Dominique Lasne, Carsten Janke, Kathiresan Natarajan, Alain Schmitt, Christine Bole-Feysot, Patrick Nitschke, Juliane Léger, Fabienne Jabot-Hanin, Frédéric Tores, Anita Michel, Arnold Munnich, Claude Besmond, Raphaël Scharfmann, François Lanza, Delphine Borgel, Michel Polak, Aurore Carré (2018 Nov 18)

TUBB1 mutations cause thyroid dysgenesis associated with abnormal platelet physiology.

EMBO molecular medicine : [DOI : e9569](https://doi.org/10.1038/s41588-018-0256-9)

Résumé

The genetic causes of congenital hypothyroidism due to thyroid dysgenesis (TD) remain largely unknown. We identified three novel gene mutations that co-segregated with TD in three distinct families leading to 1.1% of mutations in TD study cohort. (Tubulin, Beta 1 Class

VI) encodes for a member of the β -tubulin protein family. gene is expressed in the developing and adult thyroid in humans and mice. All three mutations lead to non-functional α/β -tubulin dimers that cannot be incorporated into microtubules. In mice, knock-out disrupted microtubule integrity by preventing β 1-tubulin incorporation and impaired thyroid migration and thyroid hormone secretion. In addition, mutations caused the formation of macroplatelets and hyperaggregation of human platelets after stimulation by low doses of agonists. Our data highlight unexpected roles for β 1-tubulin in thyroid development and in platelet physiology. Finally, these findings expand the spectrum of the rare paediatric diseases related to mutations in tubulin-coding genes and provide new insights into the genetic background and mechanisms involved in congenital hypothyroidism and thyroid dysgenesis.

Cáceres R, Bojanala N, Kelley LC, Dreier J, Manzi J, Di Federico F, Chi Q, Risler T, Testa I, Sherwood DR, Plastino J (2018 Nov 6)

Forces drive basement membrane invasion in *Caenorhabditis elegans*

Proceedings of the National Academy of Sciences USA : 115 : 11537-11542 : [DOI :](#)

[10.1073/pnas.1808760115](https://doi.org/10.1073/pnas.1808760115)

Résumé

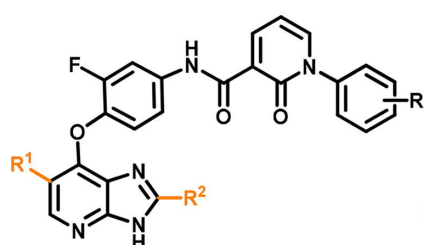
Tom Baladi, Jessy Aziz, Florent Dufour, Valentina Abet, Véronique Stoven, François Radvanyi, Florent Poyer, Ting-Di Wu, Jean-Luc Guerquin-Kern, Isabelle Bernard-Pierrot, Sergio Marco Garrido, Sandrine Piguel (2018 Nov 1)

Design, synthesis, biological evaluation and cellular imaging of imidazo[4,5-b]pyridine derivatives as potent and selective TAM inhibitors.

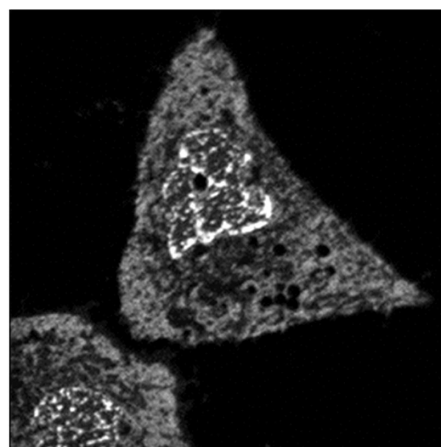
Bioorganic & medicinal chemistry : 26 : 5510-5530 : [DOI : 10.1016/j.bmc.2018.09.031](#)

Résumé

The TAM kinase family arises as a new effective and attractive therapeutic target for cancer therapy, autoimmune and viral diseases. A series of 2,6-disubstituted imidazo[4,5-b]pyridines were designed, synthesized and identified as highly potent TAM inhibitors. Despite remarkable structural similarities within the TAM family, compounds 28 and 25 demonstrated high activity and selectivity in vitro against AXL and MER, with IC value of 0.77 nM and 9 nM respectively and a 120- to 900-fold selectivity. We also observed an unexpected nuclear localization for compound 10Bb, thanks to nanoSIMS technology, which could be correlated to the absence of cytotoxicity on three different cancer cell lines being sensitive to TAM inhibition.



NanoSIMS Imaging



Cellular localisation

High activity & selectivity

IC₅₀ (TYRO3) = 270-4700 nM

IC₅₀ (AXL) = 0,77-2000 nM

IC₅₀ (MER) = 9-90 nM

Hee-Sheung Lee, Mar Carmena, Mikhail Liskovych, Emma Peat, Jung-Hyun Kim, Mitsuo Oshimura, Hiroshi Masumoto, Marie-Paule Teulade-Fichou, Yves Pommier, William C Earnshaw, Vladimir Larionov, Natalay Kouprina (2018 Nov 1)

Systematic Analysis of Compounds Specifically Targeting Telomeres and Telomerase for Clinical Implications in Cancer Therapy.

Cancer research : 78 : 6282-6296 : [DOI : 10.1158/0008-5472.CAN-18-0894](https://doi.org/10.1158/0008-5472.CAN-18-0894)

Résumé

The targeting of telomerase and telomere maintenance mechanisms represents a promising therapeutic approach for various types of cancer. In this work, we designed a new protocol to screen for and rank the efficacy of compounds specifically targeting telomeres and telomerase. This approach used two isogenic cell lines containing a circular human artificial chromosome (HAC, lacking telomeres) and a linear HAC (containing telomeres) marked with the EGFP transgene: compounds that target telomerase or telomeres should preferentially induce loss of the linear HAC but not the circular HAC. Our assay allowed quantification of chromosome loss by routine flow cytometry. We applied this dual-HAC assay to rank a set of known and newly developed compounds, including G-quadruplex (G4) ligands. Among the latter group, two compounds -Cu-ttpty and Pt-ttpty- induced a high rate of linear HAC loss with no significant effect on the mitotic stability of a circular HAC. Analysis of the mitotic phenotypes induced by these drugs revealed an elevated rate of chromatin bridges in late mitosis and cytokinesis as well as UFB (Ultrafine Bridges). Chromosome loss after Pt-ttpty or Cu-ttpty treatment correlated with the induction of telomere-associated DNA damage. Overall, this platform enables identification and ranking of compounds that greatly increase chromosome mis-segregation rates as a result of telomere dysfunction and may expedite the development of new therapeutic strategies for cancer treatment.

M Lupu, Ph Maillard, J Mispelter, F Poyer, C D Thomas (2018 Nov 1)

A glycoporphyrin story: from chemistry to PDT treatment of cancer mouse models.

Photochemical & photobiological sciences : Official journal of the European Photochemistry Association and the European Society for Photobiology : 17 : 1599-1611 : [DOI : 10.1039/c8pp00123e](https://doi.org/10.1039/c8pp00123e)

Résumé

Photodynamic therapy (PDT) represents a non-toxic and non-mutagenic antitumor therapy. The photosensitizer's (PS) chemo-physical properties are essential for the therapy, being responsible for the biological effects induced in the targeted tissues. In this study, we present the synthesis and development of some glycoconjugated porphyrins based on lectin-type receptor interaction. They were tested *in vitro* for finally choosing the most effective chemical structure for an optimum antitumor outcome. The most effective photosensitizer is substituted by three diethylene glycol α -D-mannosyl groups. *In vivo* studies allow firstly the determination of some characteristics of the biological processes triggered by the initial photochemical activation. Secondly, they make it possible to improve the therapeutic protocol in the function of the structural architecture of the targeted tumor tissue.

Annalisa Patriarca, Charles Fouillade, Michel Auger, Frédéric Martin, Frédéric Pouzoulet, Catherine Nauraye, Sophie Heinrich, Vincent Favaudon, Samuel Meyroneinc, Rémi Dendale, Alejandro Mazal, Philip Poortmans, Pierre Verrelle, Ludovic De Marzi (2018 Nov 1)

Experimental set-up for FLASH proton irradiation of small animals using a clinical system

International Journal of Radiation Oncology • Biology • Physics : 102 : 619-626 : [DOI : 10.1016/j.ijrobp.2018.06.403](https://doi.org/10.1016/j.ijrobp.2018.06.403)

Résumé**Purpose**

Recent *in vivo* investigations have shown that short pulses (FLASH) of electrons are less harmful to healthy tissues, but just as efficient as conventional dose-rate radiation to inhibit tumor growth. In view of the potential clinical value of FLASH and the availability of modern proton therapy infrastructures to achieve this goal, we herein describe a series of technological developments required to investigate the biology of FLASH irradiation, using a commercially available clinical proton therapy system.

Methods and materials

Numerical simulations and experimental dosimetric characterization of a modified clinical proton beamline, upstream from the isocenter were performed with Monte Carlo toolkit and different detectors. A single scattering system was optimized together with a ridge filter and a high current monitoring system. In addition, a submillimetric set-up protocol based on

image-guidance using a digital camera and an animal positioning system was also developed.

Results

The dosimetric properties of the resulting beam and monitoring system were characterized: linearity with dose rate and homogeneity for a 12×12 mm² field size were assessed. Dose rates exceeding 40 Gy/s at energies between 138 and 198 MeV were obtained, enabling uniform irradiation for radiobiology investigations on small animals in a modified clinical proton beam line.

Conclusion

This approach will enable us to conduct FLASH proton therapy experiments on small animals, specifically for mouse lung irradiation. Dose rates exceeding 40 Gy/s were achieved, which was not possible with the conventional clinical mode of the existing beamline.

Veronica Rodilla, Silvia Fre (2018 Nov 1)

Cellular Plasticity of Mammary Epithelial Cells Underlies Heterogeneity of Breast Cancer.

Biomedicines : [DOI : 10.3390/biomedicines6040103](https://doi.org/10.3390/biomedicines6040103)

Résumé

The hierarchical relationships between stem cells, lineage-committed progenitors, and differentiated cells remain unclear in several tissues, due to a high degree of cell plasticity, allowing cells to switch between different cell states. The mouse mammary gland, similarly to other tissues such as the prostate, the sweat gland, and the respiratory tract airways, consists of an epithelium exclusively maintained by unipotent progenitors throughout adulthood. Such unipotent progenitors, however, retain a remarkable cellular plasticity, as they can revert to multipotency during epithelial regeneration as well as upon oncogene activation. Here, we revise the current knowledge on mammary cell hierarchies in light of the most recent lineage tracing studies performed in the mammary gland and highlight how stem cell differentiation or reversion to multipotency are at the base of tumor development and progression. In addition, we will discuss the current knowledge about the interplay between tumor cells of origin and defined genetic mutations, leading to different tumor types, and its implications in choosing specific therapeutic protocols for breast cancer patients.

Arthur Charles-Orszag, Feng-Ching Tsai, Daria Bonazzi, Valeria Manriquez, Martin Sachse, Adeline Mallet, Audrey Salles, Keira Melican, Ralitzia Staneva, Aurélie Bertin, Corinne Millien, Sylvie Goussard, Pierre Lafaye, Spencer Shorte, Matthieu Piel, Jacomine Krijnse-Locker, Françoise Brochard-Wyart, Patricia Bassereau, Guillaume Duménil (2018 Oct 27)

Adhesion to nanofibers drives cell membrane remodeling through one-dimensional wetting.

Nature communications : 4450 : [DOI : 10.1038/s41467-018-06948-x](https://doi.org/10.1038/s41467-018-06948-x)

Résumé

The shape of cellular membranes is highly regulated by a set of conserved mechanisms that can be manipulated by bacterial pathogens to infect cells. Remodeling of the plasma membrane of endothelial cells by the bacterium *Neisseria meningitidis* is thought to be essential during the blood phase of meningococcal infection, but the underlying mechanisms are unclear. Here we show that plasma membrane remodeling occurs independently of F-actin, along meningococcal type IV pili fibers, by a physical mechanism that we term 'one-dimensional' membrane wetting. We provide a theoretical model that describes the physical basis of one-dimensional wetting and show that this mechanism occurs in model membranes interacting with nanofibers, and in human cells interacting with extracellular matrix meshworks. We propose one-dimensional wetting as a new general principle driving the interaction of cells with their environment at the nanoscale that is diverted by meningococci during infection.

Tanguy Lucas, Huy Tran, Carmina Angelica Perez Romero, Aurélien Guillou, Cécile Fradin, Mathieu Coppey, Aleksandra M Walczak, Nathalie Dostatni (2018 Oct 27)

3 minutes to precisely measure morphogen concentration.

PLoS genetics : e1007676 : [DOI : 10.1371/journal.pgen.1007676](https://doi.org/10.1371/journal.pgen.1007676)

Résumé

Morphogen gradients provide concentration-dependent positional information along polarity axes. Although the dynamics of the establishment of these gradients is well described, precision and noise in the downstream activation processes remain elusive. A simple paradigm to address these questions is the Bicoid morphogen gradient that elicits a rapid step-like transcriptional response in young fruit fly embryos. Focusing on the expression of the major Bicoid target, hunchback (*hb*), at the onset of zygotic transcription, we used the MS2-MCP approach which combines fluorescent labeling of nascent mRNA with live imaging at high spatial and temporal resolution. Removing 36 putative Zelda binding sites unexpectedly present in the original MS2 reporter, we show that the 750 bp of the *hb* promoter are sufficient to recapitulate endogenous expression at the onset of zygotic transcription. After each mitosis, in the anterior, expression is turned on to rapidly reach a plateau with all nuclei expressing the reporter. Consistent with a Bicoid dose-dependent activation process, the time period required to reach the plateau increases with the distance to the anterior pole. Despite the challenge imposed by frequent mitoses and high nuclei-to-nuclei variability in transcription kinetics, it only takes 3 minutes at each interphase for the MS2 reporter loci to distinguish subtle differences in Bicoid concentration and establish a steadily positioned and steep (Hill coefficient ~ 7) expression boundary. Modeling based on the cooperativity between the 6 known Bicoid binding sites in the *hb* promoter region, assuming rate limiting concentrations of the Bicoid transcription factor at the boundary, is able to capture the observed dynamics of pattern establishment but not the steepness of the

boundary. This suggests that a simple model based only on the cooperative binding of Bicoid is not sufficient to describe the spatiotemporal dynamics of early hb expression.

Abhijit Saha, Sophie Bombard, Anton Granzhan, Marie-Paule Teulade-Fichou (2018 Oct 27)

Probing of G-Quadruplex Structures via Ligand-Sensitized Photochemical Reactions in ^{Br}U-Substituted DNA.

Scientific reports : 8 : 15814 : [DOI : 10.1038/s41598-018-34141-z](https://doi.org/10.1038/s41598-018-34141-z)

Résumé

We studied photochemical reactions of ^{Br}U-substituted G-quadruplex (G4) DNA substrates with two pyrene-substituted polyazamacrocyclic ligands, M-1PY and M-2PY. Both ligands bind to and stabilize G4-DNA structures without altering their folding topology, as demonstrated by FRET-melting experiments, fluorimetric titrations and CD spectroscopy. Notably, the bis-pyrene derivative (M-2PY) behaves as a significantly more affine and selective G4 ligand, compared with its mono-pyrene counterpart (M-1PY) and control compounds. Upon short UVA irradiation (365 nm) both ligands, in particular M-2PY, efficiently sensitize photoreactions at ^{Br}U residues incorporated in G4 structures and give rise to two kinds of photoproducts, namely DNA strand cleavage and covalent ligand-DNA photoadducts. Remarkably, the photoinduced strand cleavage is observed exclusively with G4 structures presenting ^{Br}U residues in lateral or diagonal loops, but not with parallel G4-DNA structures presenting only propeller loops. In contrast, the formation of fluorescent photoadducts is observed with all ^{Br}U-substituted G4-DNA substrates, with M-2PY giving significantly higher yields (up to 27%) than M-1PY. Both ligand-sensitized photoreactions are specific to ^{Br}U-modified G4-DNA structures with respect to double-stranded or stem-loop substrates. Thus, ligand-sensitized photoreactions with ^{Br}U-substituted G4-DNA may be exploited (i) as a photochemical probe, allowing « photofootprinting » of G4 folding topologies *in vitro* and (ii) for covalent trapping of G4 structures as photoadducts with pyrene-substituted ligands.

Antoine Hocher, Myriam Ruault, Petra Kaferle, Marc Describes, Mickaël Garnier, Antonin Morillon, Angela Taddei (2018 Oct 26)

Expanding heterochromatin reveals discrete subtelomeric domains delimited by chromatin landscape transitions.

Genome research : [DOI : gr.236554.118](https://doi.org/10.1101/236554)

Résumé

The eukaryotic genome is divided into chromosomal domains of heterochromatin and euchromatin. Transcriptionally silent heterochromatin is found at subtelomeric regions, leading to the telomeric position effect (TPE) in yeast fly and human. Heterochromatin generally initiates and spreads from defined loci, and diverse mechanisms prevent the ectopic spread of heterochromatin into euchromatin. Here, we overexpressed the silencing factor Sir3 at varying levels in yeast and found that Sir3 spreads into Extended Silent Domains (ESDs), eventually reaching saturation at subtelomeres. We observed the spread of



Publications de l'UMR 168 **UMR168 - Laboratoire Physico-Chimie Curie**

Sir3 into subtelomeric domains associated with specific histone marks in wild-type cells and stopping at zones of histone mark transitions including H3K79 tri-methylation levels. Our study shows that the conserved H3K79 methyltransferase Dot1 is essential in restricting Sir3 spread beyond ESDs, thus ensuring viability upon overexpression of Sir3. Lastly, our analyses of published data demonstrate how ESDs unveil uncharacterized discrete domains isolating structural and functional subtelomeric features from the rest of the genome. Our work offers a new approach on how to separate subtelomeres from the core chromosome.